ISSN 1592-8950

AIMETA'01

XV Congresso AIMETA di Meccanica Teorica e Applicata

15th AIMETA Congress of Theoretical and Applied Mechanics

TAORMINA, 26-29 SETTEMBRE 2001

ATTI

a cura di

Giuliano AUGUSTI

Paolo Maria MARIANO Vincenzo SEPE Michele LACAGNINA

COMITATO SCIENTIFICO

G. AUGUSTI (Presidente) - *Univ. Roma "La Sapienza"*

A. M. ANILE - *Università di Catania*

G. BURESTI - *Università di Pisa*

L. CORRADI - *Politecnico di Milano*

S. DELLA VALLE - *Università di Napoli*

M. DI PAOLA - *Università di Palermo*

G. OLIVETO - *Università di Catania*

M. PANDOLFI - *Politecnico di Torino*

B. PIZZIGONI - *Politecnico di Milano*

COMITATO ORGANIZZATORE

F. PETRONE (Presidente) - *Università di Catania*

A. MORRO (Segr. AIMETA) - *Università di Genova*

G. MUSCOLINO - *Università di Messina*

S. RIZZO - *Università di Palermo*

COMITATO DIRETTIVO AIMETA

G. CAPRIZ (Presidente) - *Università di Pisa*

G. AUGUSTI - *Univ. Roma "La Sapienza"*

R. BASSANI - *Università di Pisa*

R. CONTRO - *Politecnico di Milano*

E. MARCHI - *Università di Genova*

A. MORRO - *Università di Genova*

M. PANDOLFI - *Politecnico di Torino*

SESSIONI PARALLELE

SP_GE Meccanica Generale

SP_FL Meccanica dei Fluidi

SP_MA Meccanica delle Macchine

SP_SO Meccanica dei Solidi

SP_ST Meccanica delle Strutture

SESSIONI SPECIALI

SS_ENC Energie Non Convesse in Meccanica dei Materiali

SS_MFR Meccanica della Frattura

SS_DAN Danneggiamento Meccanico nei Materiali Compositi

SS_MCO Meccanica Computazionale

INTERNATIONAL MINISYMPOSIA

MS_BIO Mechanics of Tissues and Implants

MS_MUF Multifield Theories in Mechanics of Materials

MS_INT Interaction Problems in Structural Mechanics

AIMETA '01
XV Congresso AIMETA di Meccanica Teorica e Applicata
15th AIMETA Congress of Theoretical and Applied Mechanics

A MECHANICAL MODEL FOR MIXED-MODE BUCKLING-DRIVEN DELAMINATION GROWTH

S. BENNATI[1] and P. S. VALVO[1]

[1] *Dipartimento di Ingegneria Strutturale, Università di Pisa, Pisa*

SOMMARIO
La memoria presenta un modello meccanico per la crescita di una delaminazione presente in un laminato composito, promossa da instabilità locale. Il laminato, soggetto ad un carico di compressione nel suo piano, è modellato come l'unione di due sublaminati collegati fra loro da un'interfaccia elastica, costituita da una distribuzione continua di molle elastiche lineari agenti sia nella direzione normale al suo piano sia in quella tangente. Ciò permette di determinare gli sforzi interlaminari normali e tangenziali, scambiati tra i sublaminati, e di risalire alle espressioni esplicite dei contributi dei modi I e II alla velocità di rilascio dell'energia e, conseguentemente, dell'angolo di modo misto. Alcuni primi confronti con dati sperimentali presenti in letteratura sembrano confermare l'efficacia del modello.

ABSTRACT
The paper presents a mechanical model for buckling-driven delamination growth in composite laminates. The laminate, subjected to an in-plane compressive load, is modelled as the union of two sublaminates bonded together by an elastic interface, the last being a continuous distribution of linear elastic springs acting both normally and tangentially to its plane. Hence, the normal and tangential interlaminar stresses, exerted between the sublaminates, can be deduced, and the explicit expressions for the mode-I and II contributions to the energy release rate and, consequently, the mode-mixity angle derived. A first comparison with experimental data available in the literature seems to confirm the model's effectiveness.

1. INTRODUCTION

Fibre-reinforced composite laminates are used in many civil and industrial engineering applications, where, thanks to their very high strength and stiffness and their low specific weight, they are gradually supplementing, or even replacing, traditional structural materials. On the other hand, composite laminates have also proved to be very sensitive to damage by environmental factors or localised defects. Of these latter types of damage, delaminations are both very dangerous and very common, as they may arise due to manufacturing errors (e.g., by an imperfect curing process) or in-service accidents (e.g., by low-velocity impacts) [1, 2].

When a laminated plate containing a delamination is loaded under compression, the instability phenomena that arise may promote crack growth and, in some cases, lead to failure of the whole structure. In order to model the process of combined buckling and crack growth, the methods of non-linear structural analysis can be used to deal with the equilibrium problem, while the delamination growth can be described through fracture mechanics [3, 4]. The earliest studies on the subject assumed the total potential energy release rate, G, as the parameter signalling the onset of crack growth [5, 6]. Actually, G has often been preferred to other parameters, such as stress-intensity factors, because the calculations involved are easier (e.g., by means of invariant integrals) [7]. However, experimental studies on delamination in composite laminates have shown that crack growth almost always involves the three classical modes of crack propagation: mode I, or *opening*; mode II, or *sliding*; and mode III, or *tearing*. Therefore, delamination growth is more properly described by using a mixed-mode growth criterion, whose application requires the energy release rate to be split into the sum of the contributions, G_I, G_{II} and G_{III}, of the three different propagation modes [8, 9].

The following presents a mechanical model for buckling-driven delamination growth in composite laminates, whereby a laminated plate, affected by an initial delamination and subjected to an in-plane compressive load, is represented as the union of two sublaminates bonded together by an elastic interface. This *elastic interface model* differs from analogous approaches [10, 11] in that the interface is modelled as a continuous distribution of linear elastic springs acting in both the normal and tangential directions to the interface plane [12, 13]. Hence, the normal and tangential interlaminar stresses exchanged between the sublaminates can be deduced, and the virtual crack closure technique used to derive the contributions of modes I and II to the energy release rate. Finally, the explicit expression for the mode-mixity angle, ψ, can be determined, and a mixed-mode growth criterion applied.

Kirchhoff's plate theory is used to model the above sublaminates, except for the region of the so-called 'debonded film', which is treated as a von Kármán plate in order to account for instability phenomena. Moreover, the elastic constants of the spring distributions, k_Z and k_X, are chosen in such a way as to reproduce the behaviour of the thin layer of resin joining the laminae together in a real laminate [14]. The system equilibrium is described by a non-linear differential problem, whose explicit solution has been determined in the case of a through-the-width delamination. The lengthy calculations needed to deduce this solution have been omitted here for the sake of brevity: only the final expressions are presented, along with some results in the form of graphs. However, full details can be found in [15] or in [16].

The paper closes with a comparison between the theoretical predictions stemming from the proposed model and some experimental results previously obtained by other authors [17].

2. FORMULATION OF THE PROBLEM

2.1. The model

Let us consider a rectangular laminate of length $2L$, width B, and thickness H, affected by a central, through-the-width delamination of initial length $2a$, located at a depth H_f from the nearest external surface (fig. 1). A rectangular reference system, $OXYZ$, is fixed with origin at the centre of the laminate and axes parallel to its edges. We consider the material to be homogeneous and linearly elastic. Let the orthotropy axes be aligned with those of the reference system, and let E_X, E_Y, E_Z, G_{XY}, G_{YZ}, G_{ZX}, ν_{XY}, ν_{YZ}, and ν_{ZX} be the material's elastic constants. Finally, let two compressive loads, P, act in the X-direction.

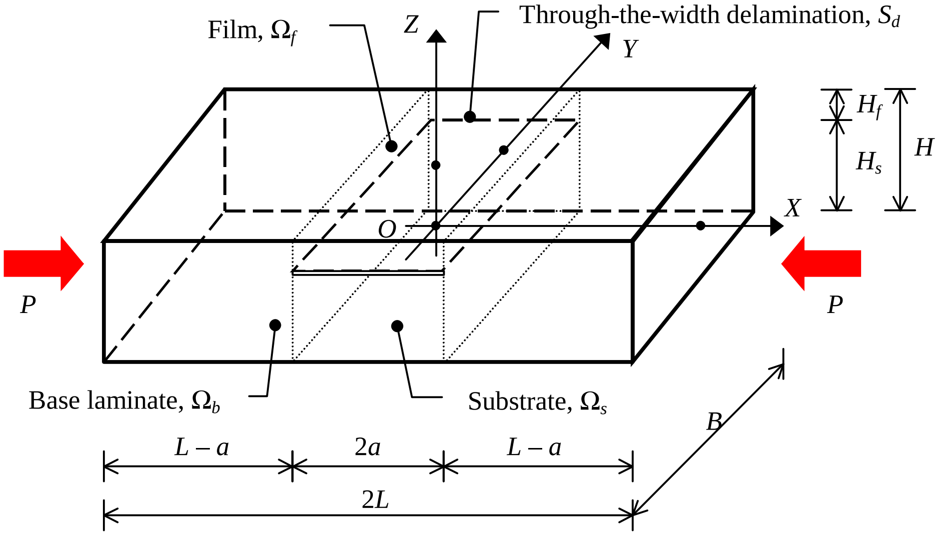

Figure 1 – Laminate with a through-the-width delamination, loaded under compression.

The model conceives of the *delaminated plate* as the union of two sublaminates, namely the *film*, included between the delamination plane and the nearest external surface and having a thickness $H_f \leq H / 2$, and the *substrate*, comprised between the delamination plane and the furthermost external surface and having a thickness $H_s = H - H_f$. Each sublaminate is further split into a *bonded* portion and a *debonded* portion (fig. 2).

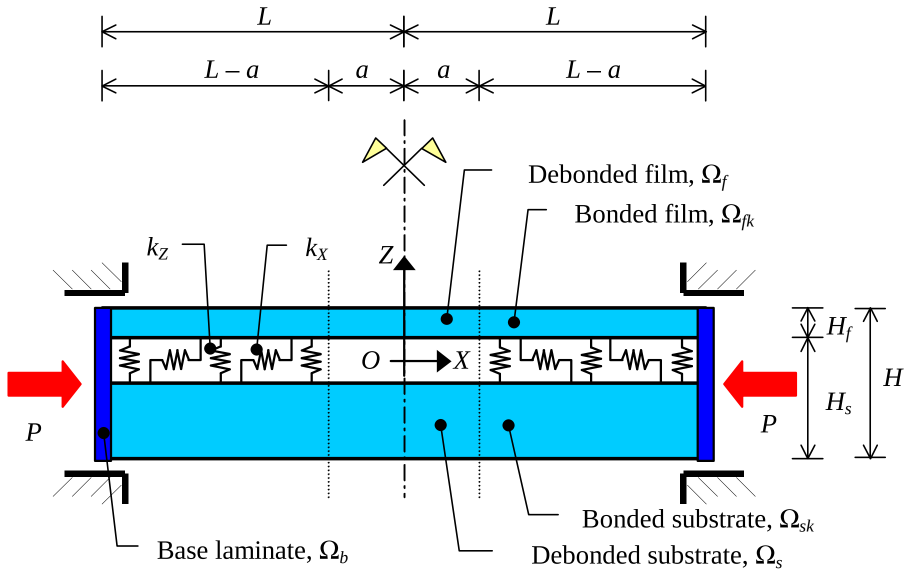

Figure 2 – The elastic interface model.

We assume that width B is 'very large', so that each sublaminate can be modelled as a *beam-plate*, i.e., as a plate with possibly non-zero curvature only in the XZ-plane. Therefore, the 'reduced' Young's modulus $E_X{*} = E_X / (1 - \nu_{XZ}\, \nu_{ZX})$ is introduced, and all calculations to follow refer to a unit width ($B = 1$). Hence, the *extensional and bending stiffnesses* of the film are $\mathsf{A}_f = E_X{*}\, H_f$ and $\mathsf{D}_f = E_X{*}\, H_f^3 / 12$, respectively; $\mathsf{A}_s = E_X{*}\, H_s$ and $\mathsf{D}_s = E_X{*}\, H_s^3 / 12$ are those of the substrate, and $\mathsf{A} = E_X{*}\, H$ and $\mathsf{D} = E_X{*}\, H^3 / 12$ are those of the base laminate. Moreover, the elastic constants of the normal and tangential springs will be denoted as k_Z and k_X, respectively.

2.2. Equilibrium equations

We suppose that the 'thick column' hypothesis holds or, in other words, that $\mathsf{D}_f << \mathsf{D}_s$ and the instability phenomenon is basically confined to the region of the debonded film Ω_f. Accordingly, von Kármán's plate theory can be adopted for modelling Ω_f, whose transverse displacements, w_f, can be moderate or large. The classical Kirchhoff plate theory is instead used for the bonded film Ω_{fk}, whose transverse displacements, w_{fk}, are considered small. Moreover, the transverse displacements of the substrate, w_s and w_{sk}, are wholly neglected, but axial displacements, u_f, u_{fk}, u_s, and u_{sk}, are accounted for in all sublaminates.

Under the above assumptions, the resulting differential equations of the equilibrium problem are

$$\frac{\partial^4 w_f}{\partial X^4} + \frac{1}{\lambda^2}\frac{\partial^2 w_f}{\partial X^2} = 0\,, \tag{1a}$$

$$\frac{\partial u_f}{\partial X} + \frac{1}{2}\left(\frac{\partial w_f}{\partial X}\right)^2 + \frac{P_f}{\mathsf{A}_f} = 0\,, \tag{1b}$$

for the debonded film Ω_f;

$$\frac{\partial^4 w_{fk}}{\partial X^4} + \frac{4}{\mu^4} w_{fk} = 0\,, \tag{2a}$$

$$\frac{\partial^2 u_{fk}}{\partial X^2} - \frac{1}{\omega^2}\frac{1}{1+\mathsf{A}_f/\mathsf{A}_s}\left(u_{fk} - u_{sk}\right) = 0\,, \tag{2b}$$

for the bonded film Ω_{fk};

$$\frac{\partial u_s}{\partial X} + \frac{P - P_f}{\mathsf{A}_s} = 0\,, \tag{3}$$

for the debonded substrate Ω_s; and

$$\frac{\partial^2 u_{sk}}{\partial X^2} + \frac{1}{\omega^2}\frac{1}{1+\mathsf{A}_s/\mathsf{A}_f}\left(u_{fk} - u_{sk}\right) = 0\,, \tag{4}$$

for the bonded substrate Ω_{sk}.

In the above expressions, P_f is the *buckling load of the debonded film* (to be determined as explained in the following) and λ, μ and ω are *auxiliary constants*, defined by:

$$\lambda^2 = \frac{\mathsf{D}_f}{P_f}\,, \qquad \mu^4 = 4\frac{\mathsf{D}_f}{k_Z}\,, \qquad \omega^2 = \frac{1}{k_X}\frac{1}{1/\mathsf{A}_f + 1/\mathsf{A}_s}\,. \tag{5a,b,c}$$

The differential problem is completed by appropriate boundary conditions, which include the symmetry condition on the YZ-plane (only a half plate is considered in the calculations) and the clamped-end condition at the loaded end of the laminate.

3. SOLUTION OF THE PROBLEM

3.1. Equilibrium in the post-critical phase

The stated equilibrium problem can be solved completely in explicit form [15, 16]. For brevity's sake, here we limit ourselves to presenting the final expressions only. In particular, the expressions for the *transverse displacements* of the film in the post-critical phase are

$$w_f = A_f\left(\cos\frac{X}{\lambda} + d_f\right), \tag{6a}$$

$$\begin{aligned} w_{fk} = A_f\Bigg[&\left(a_{fk}\cosh\frac{X-a}{\mu} + b_{fk}\sinh\frac{X-a}{\mu}\right)\cos\frac{X-a}{\mu} + \\ &+\left(c_{fk}\cosh\frac{X-a}{\mu} + d_{fk}\sinh\frac{X-a}{\mu}\right)\sin\frac{X-a}{\mu}\Bigg], \end{aligned} \tag{6b}$$

where A_f is the amplitude of the sinusoid representing the transverse displacement of Ω_f, and d_f, a_{fk}, b_{fk}, c_{fk}, and d_{fk} are dimensionless integration constants (see [13] for their expressions).

Likewise, the expressions for the *axial displacements* in the four sublaminates are

$$u_f = -\frac{P_C}{\mathsf{A}}X - \frac{A_f^2}{8\lambda}\left(\frac{2X}{\lambda} - \sin\frac{2X}{\lambda}\right), \tag{7a}$$

$$\begin{aligned} u_{fk} = &-\frac{P}{\mathsf{A}}X + \frac{P-P_C}{\mathsf{A}}\left(a\cosh\frac{X-a}{\omega} + \omega\sinh\frac{X-a}{\omega}\right) + \\ &-\frac{A_f^2}{8\lambda}\left(\frac{2a}{\lambda} - \sin\frac{2a}{\lambda}\right)\left(\frac{\mathsf{A}_s}{\mathsf{A}}\cosh\frac{X-a}{\omega} + \frac{\mathsf{A}_f}{\mathsf{A}}\right), \end{aligned} \tag{7b}$$

$$u_s = -\frac{1}{\mathsf{A}_s}\left(P - \frac{\mathsf{A}_f}{\mathsf{A}}P_C\right)X, \tag{7c}$$

$$\begin{aligned} u_{sk} = &-\frac{P}{\mathsf{A}}X - \frac{\mathsf{A}_f}{\mathsf{A}}\frac{P-P_C}{\mathsf{A}_s}\left(a\cosh\frac{X-a}{\omega} + \omega\sinh\frac{X-a}{\omega}\right) + \\ &+\frac{\mathsf{A}_f}{\mathsf{A}}\frac{A_f^2}{8\lambda}\left(\frac{2a}{\lambda} - \sin\frac{2a}{\lambda}\right)\left(\cosh\frac{X-a}{\omega} - 1\right), \end{aligned} \tag{7d}$$

where $P_C = P_f\,(\mathsf{A} / \mathsf{A}_f)$ is the *buckling load of the delaminated plate*, i.e., the load applied to the laminate upon incipient buckling of the debonded film. By putting expressions (6) and (7) into the boundary conditions, a set of linear homogeneous algebraic equations for the six unknown integration constants is obtained. For a nontrivial solution to exist, its *determinant*,

$$\begin{aligned} \det\mathbf{R} = -\frac{2}{\lambda^3\mu^5}\sec^2\frac{L-a}{\mu}\Bigg\{&2\lambda\mu\left(\operatorname{sech}^2\frac{L-a}{\mu}\sin\frac{L-a}{\mu}\cos\frac{L-a}{\mu} + \tanh\frac{L-a}{\mu}\right)\cos\frac{a}{\lambda} + \\ &+\left[\left(2\lambda^2+\mu^2\right)\operatorname{sech}^2\frac{L-a}{\mu}\cos^2\frac{L-a}{\mu} + 2\lambda^2 - \mu^2\right]\sin\frac{a}{\lambda}\Bigg\}, \end{aligned} \tag{8}$$

must vanish. Thus, the buckling load, P_C, is found numerically by imposing det $\mathbf{R} = 0$.

Next, the integration constants can be determined explicitly and, in particular, the *amplitude* of the film's transverse displacement,

$$A_f = \sqrt{\frac{8\lambda}{2a/\lambda - \sin(2a/\lambda)}\left(a + \omega \tanh\frac{L-a}{\omega}\right)\frac{P - P_C}{\mathsf{A}_s}}\,, \tag{9}$$

which is zero throughout the pre-critical phase, becomes an increasing function of the applied load only after buckling has occurred.

For the purposes of illustration, the subsequent numerical values have been chosen to render the figures provided: $L = 100$ mm, $H = 10$ mm and $H_f = 1$ mm; $E_X = 54$ GPa, $E_Y = 18$ GPa, $G_{XY} = 9$ GPa and $\nu_{XY} = 0.250$. Moreover, loads have been made dimensionless by dividing by the Euler load, $P_{EUL} = \pi^2\, \mathsf{D} / L^2 = 4535.8$ N/mm (which is the buckling load of the undamaged plate), and the delamination half-length, a, has been divided by the plate length, L.

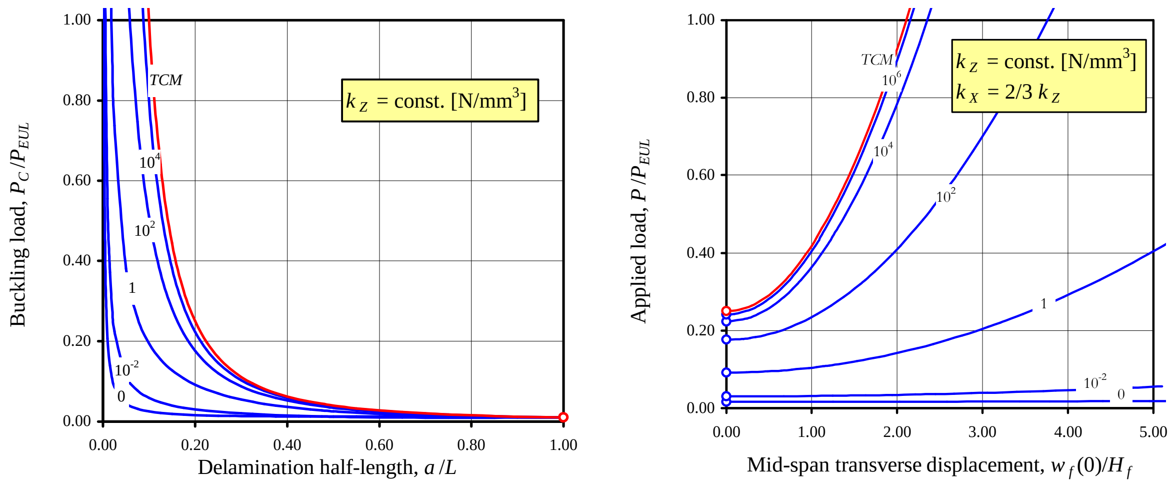

a) b)

Figure 3 – Post-critical equilibrium: a) buckling load of the delaminated plate vs. delamination half-length; b) applied load vs. mid-span transverse displacement of the film.

The curves in figure 3a represent the buckling load, P_C, as a function of the delamination half-length, a, for a range of values of the normal spring constant, k_Z. As expected, P_C is a decreasing function of a. As $a/L \to 0$ (no delamination), the predicted buckling loads tend to infinity, a consequence of having neglected the instability of the bonded film. However, values of $P_C/P_{EUL} > 1$ have no physical meaning and must therefore be excluded. Instead, as $a/L \to 1$ (complete delamination), $P_C \to P_f^L\,(\mathsf{A} / \mathsf{A}_f)$, where $P_f^L = \pi^2\, \mathsf{D}_f / L^2 = 4.5$ N/mm is the buckling load of the completely debonded film.

Moving on to examine the post-critical behaviour, we assume a fixed delamination half-length, $a = 20$ mm. Figure 3b shows the applied load vs. the transverse displacement of the mid-span section of the debonded film, $w_f(0)$, made dimensionless by dividing by H_f. A range of values for the normal spring constant, k_Z, has been considered, while the tangential spring constant has been set at $k_X = 2/3\, k_Z$.

It is worth noting that as $k_Z \to \infty$, the predictions of the elastic interface model (blue curves) approach those of the *thick column model (TCM)* [6] (red curves). The *elastic constants* of the interface can be chosen as

$$k_Z = \frac{E_r}{t}, \quad \text{and} \quad k_X = \frac{2G_r}{t}, \tag{10}$$

where E_r and G_r are the elasticity moduli of the resin, and t is the thickness of the lamina [14]. In the following, we have assumed E_r = 3.5 GPa, G_r = 1.3 GPa and t = 0.15 mm. In general, it is reasonable to expect that $k_Z = 10^4 \div 10^6$ N/mm^3 and $k_X / k_Z = 2/3 \div 1$.

3.2. Delamination growth

Once the transverse and axial displacement have been determined, it is possible to arrive at the explicit expressions for the normal and tangential *interlaminar stresses*:

$$\begin{aligned}\sigma_{ZZ} = k_Z A_f \Bigg[&\left(a_{fk} \cosh \frac{X-a}{\mu} + b_{fk} \sinh \frac{X-a}{\mu} \right) \cos \frac{X-a}{\mu} + \\ &+ \left(c_{fk} \cosh \frac{X-a}{\mu} + d_{fk} \sinh \frac{X-a}{\mu} \right) \sin \frac{X-a}{\mu} \Bigg],\end{aligned} \tag{11a}$$

$$\tau_{ZX} = -k_X \frac{P - P_C}{A_s} \omega \left(\tanh \frac{L-a}{\omega} \cosh \frac{X-a}{\omega} - \sinh \frac{X-a}{\omega} \right), \tag{11b}$$

Figures 4a and 4b, respectively, show the two foregoing stress components as functions of the abscissa, X, for increasing load levels. Both components reach a maximum at the delamination front and then undergo rapid decay as X increases.

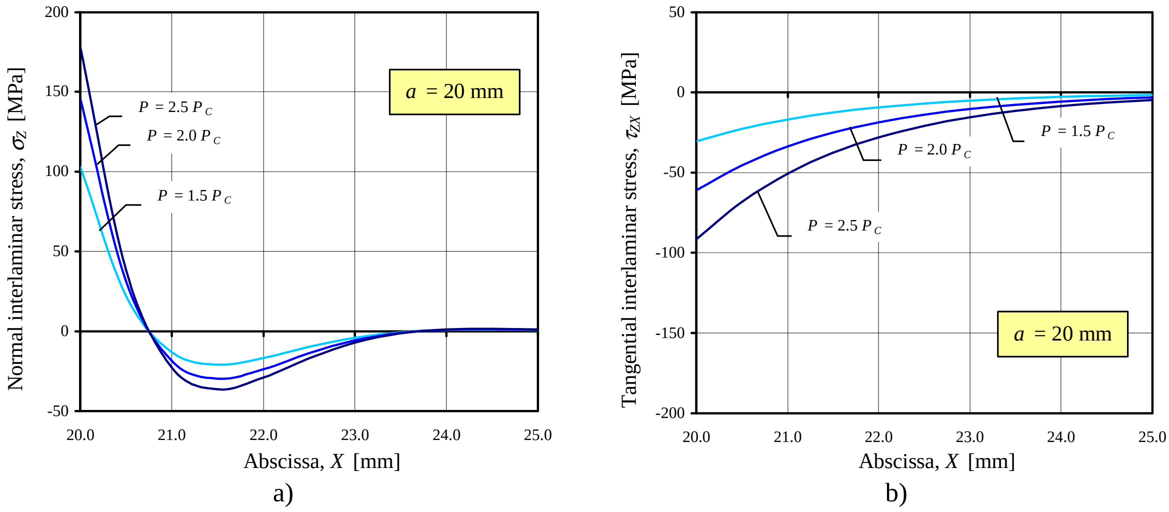

Figure 4 – Interlaminar stresses at the delamination front: a) normal stress; b) tangential stress.

Griffith's classical crack growth criterion, however, is not expressed directly in terms of interlaminar stresses. Rather, it assumes that crack growth takes place when the *energy release rate*, $G = -\partial\Pi / \partial a$ (where Π is the *total potential energy* of the system) reaches a critical value, G_C. In its original and simplest formulation, G_C is a material constant to be determined by experiment. Nevertheless, for anisotropic and inhomogeneous materials, such as composite laminates, it is an established fact that experimental determinations of G_C are markedly dependent on the *propagation mode* (I or *opening*, II or *sliding*, III or *tearing*) operative in the test performed. Actually, the critical value measured in a pure mode-III test, $G_{III\,C}$, is usually greater than that obtained in a pure mode-II test, $G_{II\,C}$, which may, in turn, be much greater than the value measured in a pure mode-I test, $G_{I\,C}$.

Under *mixed-mode* conditions, i.e., when all propagation modes are simultaneously operative, an intermediate value of G_C is to be expected, depending on which mode prevails. In these cases, a so-called *mixed-mode criterion* is to be adopted by considering G_C to be, rather than a constant, a function of the relative amount of the different propagation modes. For plane problems, for which mode III is irrelevant, a possible definition of the *critical energy release rate* is:

$$G_C(\psi) = \frac{G_{I\,C}}{1 + (\lambda_2 - 1)\sin^2\psi}, \tag{12}$$

where the ratio $\lambda_2 = G_{I\,C}/G_{II\,C}$ has been introduced, together with the *mode-mixity angle*,

$$\psi = \arctan\left|\frac{\tau_{ZX}(a)}{\sigma_{ZZ}(a)}\right|, \tag{13}$$

which conventionally measures the relative amount of mode II with respect to mode I, by ranging from 0° (pure mode-I conditions) to 90° (pure mode-II conditions) [9].

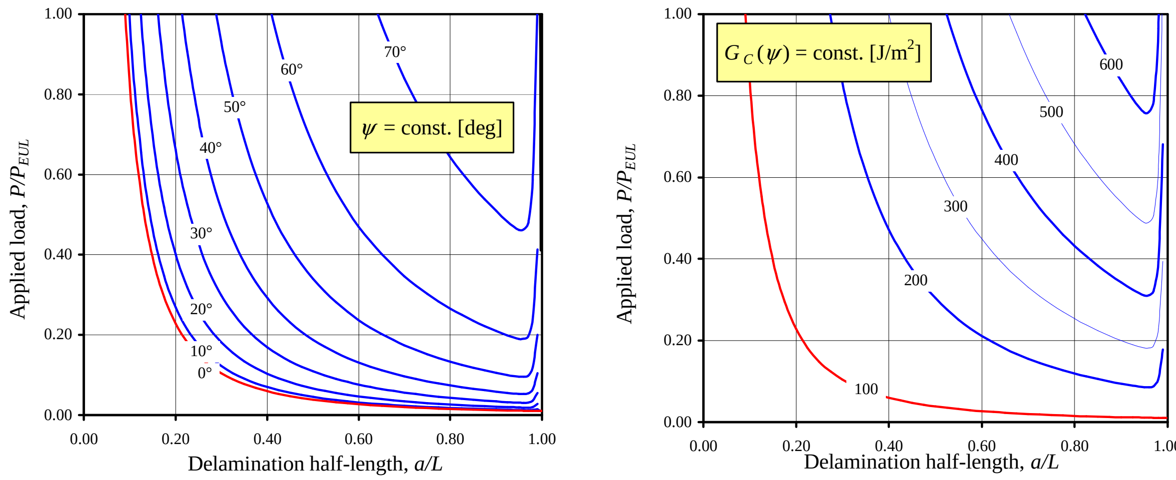

a) b)

Figure 5 – Mixed-mode criterion: a) mode-mixity angle; b) critical energy release rate.

A main difficulty in modelling the processes of combined delamination buckling and growth is that the mode mixity is not fixed once and for all, but undergoes a characteristic evolution. As a fundamental result of the present model, the contour plot of ψ has been obtained (fig. 5a): it shows that the mode-mixity angle is zero upon incipient buckling (red curve) and then increases as either the applied load or the delamination length grows. Hence, a transition from the opening (I) to the sliding mode (II) occurs as the process itself develops.

Figure 5b represents the contour plot of the mixed-mode critical energy release rate, computed according to definition (12) and assuming $G_{I\,C} = 100$ J/m^2 and $G_{II\,C} = 1000$ J/m^2. It should be stressed that upon buckling (red curve), pure mode-I conditions exist and, consequently, $G_C(\psi) = G_{IC}$; instead, as ψ increases, $G_C(\psi)$ increases significantly as well (for $\psi = 90°$, it would be equal to G_{IIC}).

The potential energy release rate, G, now remains to be determined. According to the virtual crack closure technique, G is the sum of the *modal contributions*,

$$G_I = \lim_{\Delta a \to 0} \frac{1}{2\Delta a} \int_a^{a+\Delta a} \Delta\hat{w}\left(\hat{X} - \Delta a\right) \sigma^*_{ZZ}(X)\, dX\,, \tag{14a}$$

$$G_{II} = \lim_{\Delta a \to 0} \frac{1}{2\Delta a} \int_a^{a+\Delta a} \Delta\hat{u}\left(\hat{X} - \Delta a\right) \tau^*_{ZX}(X)\, dX\,, \tag{14b}$$

where the hat (^) refers to a plate in which the delamination has experienced a ‘virtual’ growth by a length Δa, and the asterisk (*) denotes the effective system. By substituting relations (6), (7) and (11) into (14) and performing the calculations, the following results are obtained:

$$G_I = \frac{1}{2} k_Z a_{fk}^2 \frac{8\lambda}{2a/\lambda - \sin(2a/\lambda)} \left(a + \omega \tanh\frac{L-a}{\omega} \right) \frac{P - P_C}{\mathsf{A}_s}\,, \tag{15a}$$

$$G_{II} = \frac{1}{2} k_X \left(\omega \tanh\frac{L-a}{\omega} \frac{P - P_C}{\mathsf{A}_s} \right)^2 . \tag{15b}$$

Figures 6a and 6b show the contour plots of the mode-I and II contributions to the energy release rate, G_I and G_{II}, respectively. Clear differences emerge in the qualitative trends of the two families of curves. In fact, along the G_I-contour lines, the applied load, P, is initially a decreasing function of a; it then reaches a minimum and afterwards becomes an increasing function. Consequently, if a pure mode-I growth criterion were assumed ($G_I = G_{IC}$), then *stable growth* would be predicted for delamination lengths greater than a certain value, corresponding to that minimum. On the contrary, along the G_{II}-contour lines, the applied load, P, is a decreasing function of a, nearly up to $a = L$, so that a pure mode-II criterion ($G_{II} = G_{IIC}$) would predict *unstable growth* until complete delamination ensues.

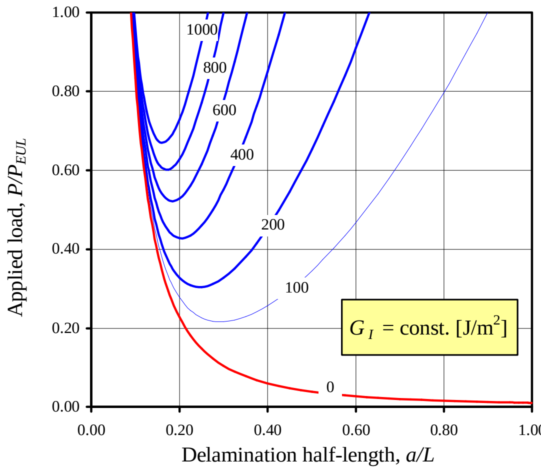

a)

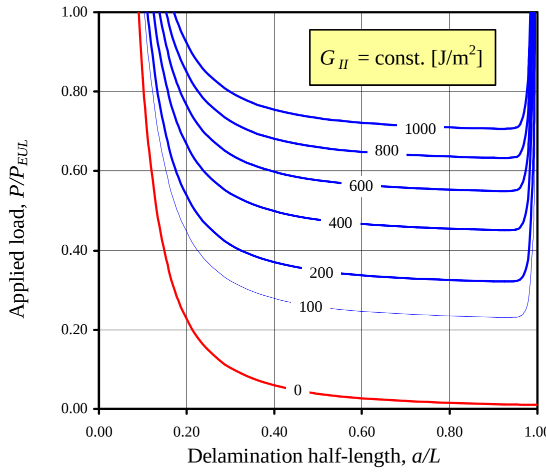

b)

Figure 6 – Potential energy release rate: a) mode-I contribution; b) mode-II contribution.

Likewise, along the contour lines of the total energy release rate, $G = G_I + G_{II}$ (fig. 7a), the applied load, P, is initially a decreasing function of a, and then reaches a minimum, after which it becomes an increasing function. However, in this case the increasing trend is very weak, so that adopting Griffith's classical growth criterion ($G = G_C$ = const.) would predict *stable growth*, but only in theory, as very small increments in P would suffice to promote complete delamination.

Figure 7b shows two curves summarising the main results obtained so far through the proposed model: the red is the *buckling curve*, defined by $P = P_C(a)$, which indicates the beginning of instability phenomena; the blue is the *growth curve*, defined by $G = G_C(\psi)$, which represents the process of delamination growth. Two important values of the delamination half-length have been highlighted in the figure: a_1, at which $P_C = P_{EUL}$, and a_2, at which the applied load along the growth curve reaches a minimum. The mechanical interpretation of these values is as follows: if the length of the delamination is such that $a < a_1$, local buckling phenomena and related delamination growth are not to be expected (although global instability can still occur!); if, on the other hand, $a_1 < a < a_2$, delamination buckling and growth will both be possible, the latter resulting in an unstable process; finally, if $a_2 < a$, then delamination buckling and growth will once again be possible, but the latter will be a stable process.

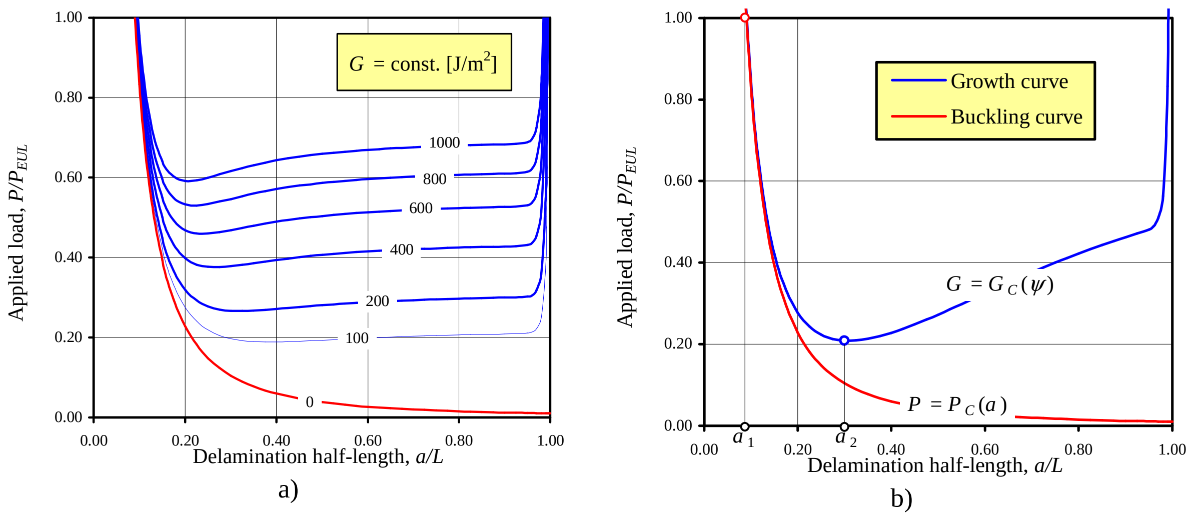

Figure 7 – Delamination growth: a) total energy release rate; b) buckling and growth curve.

4. CONCLUDING REMARKS

In the foregoing we have set forth a mechanical model, termed the *elastic interface model*, for buckling-driven delamination growth in composite laminates. Despite its apparent simplicity, which enables arriving at an explicit solution, the model appears able to furnish a number of relevant predictions regarding both the system equilibrium in the pre- and post-critical phases, and the process of delamination growth and its stability, while also accounting for mixed-mode propagation.

However, considering, amongst other aspects, the many simplifying assumptions introduced, one might suspect the foregoing results to be merely theoretical and, therefore, of little practical interest as far as applications are concerned. In order to mitigate such doubts, the model's predictions have been subjected to a first validation through comparison with some available experimental data.

For the sake of this comparison, figure 8a has been drawn from a wide-ranging experimental study on graphite-epoxy laminates affected by through-the-width delaminations [17]. The figure shows the strains, ε_f and ε_s, for increasing load levels as measured by two strain-gauges glued to opposite sides of a specimen, corresponding to the film and the substrate, respectively. Three phases of the specimen's response can be clearly discerned: in the first phase, relative to pre-critical behaviour, the load-strain curve is almost linear; thereafter, a bifurcation point is reached and a second phase, corresponding to post-critical behaviour, follows; finally, a third phase, associated with delamination growth, is observed, where abrupt discontinuities in the strain measures appear prior to failure of the specimen.

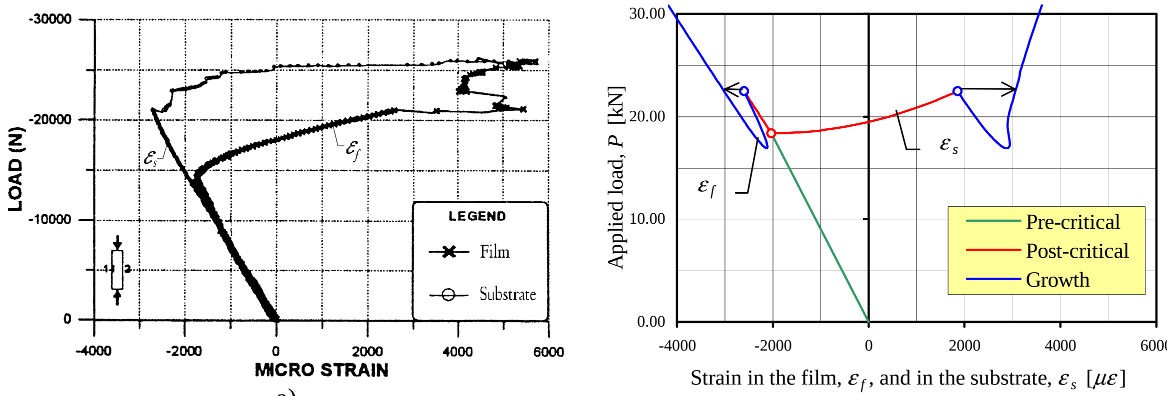

a) b)

Figure 8 – Load-strain plot for a small delamination ($2a$ = 19.05 mm): a) experimental; b) theoretical.

Figure 8b shows the predictions of the elastic interface model for the same case using the numerical values adopted in the cited paper: $2L$ = 50.8 mm, B = 25.4 mm, H = 2.54 mm and H_f = 0.51 mm; E_X = 139.3 GPa, E_Y = 9.72 GPa, G_{XY} = 5.59 GPa and ν_{XY} = 0.29; E_r = 3.5 GPa, G_r = 1.3 GPa and t = 0.127 mm; $G_{I\,C}$ = 193 J/m^2 and $G_{II\,C}$ = 455 J/m^2. Moreover, in line with classical laminated plate theory, A_f = 71182 N/mm and D_f = 1531 N mm^2, and relations (10) yield k_Z = 28000 N/mm^3 and k_X = 20000 N/mm^3. The theoretical predictions match the experimental data both qualitatively and quantitatively. There is, in particular, a very good correspondence between the two determinations of the bifurcation point. Finally, it is worth noting that during the growth phase, a sort of snap-through phenomenon is predicted, which might serve as an explanation for the discontinuities in the strain-gauge measures.

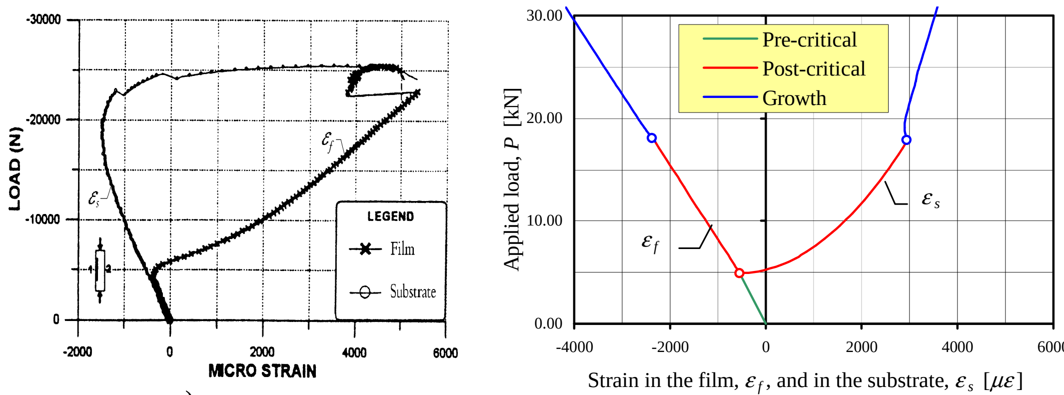

a) b)

Figure 9 – Load-strain plot for a large delamination ($2a$ = 38.10 mm): a) experimental; b) theoretical.

Figures 9a and 9b refer to a larger initial delamination length. Once again in this case, the theoretical and experimental results agree quite closely. The main discrepancy regards the values reported by the strain-gauge fixed on the thicker side of the laminate: because of global buckling, during the post-critical phase the measured strains retrieve a part of the compressive (negative) deformation and, after a certain load level, even become positive. Such behaviour cannot be foreseen by the model, which completely disregards bending of the substrate.

The last aspect, as well as many others such as a more general plate geometry and a stronger material anisotropy, no doubt deserves further investigation. However, the promising results obtained up to now give good reason to hope in the success of future studies.

REFERENCES

[1] Garg A. C.: «Delamination – A damage mode in composite structures», *Engineering Fracture Mechanics*, Vol. 29, pp. 557-584 (1988).

[2] Abrate S.: «Impact on laminated composite materials», *Appl. Mech. Reviews*, Vol. 44, pp. 155-190 (1991).

[3] Storåkers B.: «Nonlinear aspects of delamination in structural members», *ICTAM '89, 17th International Congress of Theoretical and Applied Mechanics*, Grenoble, France, 1988, pp. 315-336; North-Holland, Elsevier Science Publishers, Amsterdam, 1989.

[4] Bolotin V. V.: «Delaminations in composite structures: its origin, buckling, growth and stability», *Composites Part B: Engineering*, Vol. 27, pp. 129-145 (1996).

[5] Kachanov L. M.: Delamination buckling of composite materials; Kluwer Academic Publishers, Dordrecht-Boston-London, 1988.

[6] Chai H., Babcock C. D., Knauss W. G.: «One dimensional modelling of failure in laminated plates by delamination buckling», *Int. J. of Solids and Structures*, Vol. 17, pp. 1069-1083 (1981).

[7] Yin W.-L., Wang, J. T.-S.: «The energy-release rate in the growth of a one-dimensional delamination», *Trans. ASME, J. of Applied Mechanics*, Vol. 51, pp. 939-941 (1984).

[8] Whitcomb J. D.: «Finite element analysis of instability related delamination growth», *J. of Composite Materials*, Vol. 15, pp. 403-426 (1981).

[9] Hutchinson J. W., Suo Z.: «Mixed mode cracking in layered materials», *Advances in Applied Mechanics*, Vol. 29, pp. 63-191 (1992).

[10] Vizzini A. J., Lagace P. A.: «The buckling of a delaminated sublaminate on an elastic foundation», *J. of Composite Materials*, Vol. 21, pp. 1106-1117 (1987).

[11] Bruno D., Grimaldi A.: «Delamination failure of layered composite plates loaded in compression», *Int. J. of Solids and Structures*, Vol. 26, pp. 313-330 (1990).

[12] Point N., Sacco E.: «A delamination model for laminated composites», *Int. J. of Solids and Structures*, Vol. 33, pp. 483-509 (1996).

[13] Bennati S., Valvo P. S.: «An elastic-interface model for delamination buckling», *Key Engineering Materials*, in press (2001).

[14] Corigliano A.: «Formulation, identification and use of interface models in the numerical analysis of composite delamination», *Int. J. of Solids and Structures*, Vol. 30, pp. 2779-2811 (1993).

[15] Valvo P. S.: Fenomeni di instabilità e di crescita della delaminazione nei laminati compositi; Tesi di Dottorato, Università degli Studi di Firenze, 2000.

[16] Bennati S., Valvo P. S.: «A simple mechanical model describing delamination buckling and mixed-mode growth in composite laminates», *Int. J. of Solids and Structures*, to be submitted.

[17] Lee Y. J., Lee C.H., Fu W. S.: «Study on the compressive strength of laminated composite with through-the-width delamination», *Composite Structures*, Vol. 41, pp. 229-241 (1998).